International Journal of Engineering

Journal Homepage: www.ije.ir

Towards a Uncertainty Analysis in Thermal Protection using Phase-change Micro/Nano Particles during Hyperthermia

A. A. Taheri*, M. Taghilou

Department of Mechanical Engineering, Faculty of Engineering, University of Zanjan, Zanjan, Iran

P A P E R I N F O

Paper history:
Received 25 August 2020
Received in revised form 25 September 2020
Accepted 30 October 2020

Keywords:
Electromagnetic Field
Hyperthermia
Phase-Change Micro/Nano Martials
Superparamagnetic Micro/Nano Particles
Uncertainty Analysis

A B S T R A C T

In thermal protection of healthy tissues during hyperthermia with the phase-change micro/nano-materials, the impossibility of performing a similar experiment with the theoretical parameters is inevitable because of different errors such as modeling, measuring, particle deposition area, etc. These errors may affect the practical thermal protection from damaging the healthy tissue or not destroying the tumor tissue. To perform a numerical procedure, the electrical potential is obtained solving the Laplace equation and the Pennes Biothermal equation is used to find the temperature distribution in the tissue using the finite difference method. The Pennes equation is transiently resolved by considering intracellular conductance, blood perfusion, and metabolic heating. Consequently, the deviation and the uncertainty of each parameters in the thermal protection including the concentration of the phase change material, the radius of microcapsules, the latent heat, the melting point, the temperature range of phase change of micro/nanoparticles, and the concentration and the radius of the superparamagnetic materials are investigated. According to the results of the uncertainty analysis, the radius of the superparamagnetic materials is the most important parameter so that a 20% deviation from the numerical value changes the temperature of the tissue up to 4 °C.

doi: *10.5829/ije.2021.34.01a.29*

1. INTRODUCTION

Based on the statistics released by the International Agency for Research on Cancer (IARC), about 110,000 cases of cancer occurred in Iran and about 56,000 of them have passed away [1]. These statistics demonstrate the importance of research on cancer and its treatment [2-4]. Hyperthermia that is known as thermotherapy is a technique for cancer treatment. In this treatment, cancerous tissue or the whole body through the use of electromagnetic energy are exposed to temperatures between 41-43 ºC to damage or kill the cancer cells. Higher than this temperature range, the heat would kill tumor and healthy cells, and this known as thermal ablation. Nowadays, hyperthermia is always used together with other forms of cancer treatment methods which allows more synergy with different proceedings of conventional treatments [5].

The treatment of cancer, based on nanotechnology is a specific form of interstitial thermotherapy with the advantage of selective heat deposition to the tumor cells [6]. This technique is made by the injection of Super-Paramagnetic Materials (SPMs) into the tumor tissue and then applying an external magnetic field which leads to heat generation. Delivery of the treatment agent to the target area is the key points to effective treatment [7]. Despite the advantage of selective heat deposition, overheating of healthy tissues are possible that could cause burn, blister, and pain [6, 8]. The electromagnetic field can itself, causes cancer depending on how they are produced [9] or improve body behavior [10]. Also, the nanoparticles should not have a toxic effect on the body [11, 12]. Cobalt ferrite (CoFe2O4) is one of these nanoparticle that can be used in hyperthermia [13].

Phase-Change Materials (PCMs) store energy at a constant temperature so that, an increase in tissue temperature during the hyperthermia will be low. Additionally, because of the low thermal conductivity of the PCMs, they prevent heat conduction from the cancerous tissues to the healthy tissues [14]. Sezgin et al.

*Corresponding Author Email: *aliasghartaheri310@gmail.com* (A. A. Taheri)

Please cite this article as: A. A. Taheri, M. Taghilou, Towards a Uncertainty Analysis in Thermal Protection using Phase-change Micro/Nano Particles during Hyperthermia, International Journal of Engineering, Transactions A: Basics, Vol. 34, No. 1, (2021) 263-271

[15] investigated hyperthermia in combination with chemotherapy mediated by gold nanoparticles. They concluded that the presence of nanoparticles increases the treatment efficacy. Lv et al. [14] injected the PCM around the tumor by the goal of protecting healthy tissues during the hyperthermia. The results showed that the PCM can significantly reduce the temperature around the tumor tissue. Lv et al. [16] also proposed a new model for utilizing of the micro/nanomaterials in the living tissue using Monte Carlo's method. Deng and Liu [17] investigated uncertainty analysis during induction hyperthermia using SPM. They concluded that uncertainty analysis should be applied when designing the treatment plan. Majchrzak et al. [18] studied induction hyperthermia with choosing a two dimensional model and applying the electromagnetic field using Boundary Element Method (BEM). They examined different voltages and frequencies and showed that the optimum value for these parameters must be determined to achieve the optimal treatment.

Majchrzak and Paruch [19, 20] applied the Finite Element Method (FEM) to examine the effect of location and size of the external electrodes on the temperature distribution in the tumor tissue. Zhao et al. [21] conducted a study about hyperthermia using magnetic nanoparticles on the laboratory mice. Experimental results showed that within the first 5-10 minutes the temperature of the tumor center reached about 40 ºC. Taheri and Talati [22] obtained the temperature distribution in the tissue by injecting electromagnetic micro/nanomaterials and then applying the electromagnetic field. The results showed that inserting the nanoparticles into the tumor significantly increases the temperature in this tissue and transmits the maximu m temperature to the tumor center. Taheri and Talati [23] also investigated the uncertainty of the effective parameters during hyperthermia with SPM nanoparticles. They concluded that uncertainties in the measurement of some parameters, such as strength of electromagnetic field, radius, and area of the micro/nanoparticle severely affect the temperature distribution in the tissue. In other work, Taheri and Talati [24] examined the hyperthermia cancer treatment by considering the two-dimensional transient model of biological tissue with SPM and PCM. Results showed that the use of the PCM reduces the temperatures up to 3°C. Nemati et al. [25] showed that by deforming the spherical SPMs into the cubes (octopods) ones, their specific rate of absorption could be increased by 70%. Wang et al. [26] obtained an optimal temperature distribution for a 3D triple-layered skin structure that is embedded with multi-level blood vessels considering electromagnetic radiation heat source. The effects of geometric structures of vascular trees and blood flow are investigated by Li et al. [27]. They derived a fractal model for the effective thermal conductivity of the living biological tissue and found that the blood flow highly affects the effective thermal conductivity. Despite the thermal protection of PCMs, the incompatibility of the practical parameters with the numerical estimations could make it problematic for the treatment procedure. Therefore, for designing a decent therapeutic pattern in laboratory conditions, the possible deviations from the numerical values should be examined.

In this study, the deviation and the uncertainty analysis of each effective parameters in thermal protection including the concentration, the radius of microcapsules, the latent heat, the melting point, the temperature range of phase change of micro/nanoparticles, and also the effect of the concentration and the radius of superparamagnetic materials are investigated. For this purpose, the distribution of electrical potential within the tissue is first obtained using Laplace equation. As the potential distribution is determined, the heat production in the different regions of the tissue will be obtained. This heat, together with the metabolic heat of the body, enters into the biothermal equation of Pennes. This equation provides a transient temperature distribution in the tissue, taking into account the conductivity of the tissue as well as blood perfusion. After determining the temperature distribution, the uncertainties of each of the important parameters with a 20% tolerance have been investigated.

The rest of the paper has been compiled in this way. Section 2 expresses the problem geometry with details of the governing equations. Uncertainty analysis is defined in section 3 and numerical procedure with mesh independency and verification tests are provided in section 4. Numerical results are presented in section 5 and general conclusions are given in section 6.

2. THEORETICAL MODEL

Here, three regions with different properties including healthy tissue without PCM, tumor with SPMs, and healthy tissue with PCMs are considered. Figure 1 shows these regions by Ω_1, Ω_2, and Ω_3, respectively.

To prevent damage caused by overheating, two pads cool down the surface of the skin. Also, paraffin wax with a melting temperature of 38-42 ºC is assumed as the PCM and injected around the tumor with high concentration (see Figure 1). Details of geometric information and thermophysical properties of three regions are reported in section 5. If the permittivity of the dielectric is constant, the potential within the tissue, φ could be determined using the Laplace equation [16]:

$$\nabla^2\varphi(x,y)=0 \tag{1}$$

$$\varphi(x,y)=\pm U, \qquad (x,y)\in\Omega_h$$
$$\frac{\partial\varphi(x,y)}{\partial q}=0, \qquad (x,y)\notin\Omega_h \tag{2}$$

where U is the voltage of the electrodes, q is the direction normal to the boundaries, and Ω_h is area of the electrodes. The strength of the electric field is determined as [16]:

$$\mathbf{E}(x,y) = -\nabla\varphi(x,y) \tag{3}$$

Heat generation in the tissues without SPM particles depends on the electrical conductivity and strength of the electric field $\boldsymbol{E}$. Thus, volumetric heat generation in these regions could be determined for electric field $\boldsymbol{E}$, roughly [16]:

$$Q_r = \sigma_i \frac{|\mathbf{E}(x,y)|^2}{2} = \frac{\sigma_i\left[|E_x|^2 + |E_y|^2\right]}{2} \quad (x,y) \in \Omega_{1,3}. \tag{4}$$

where σ_i is the electrical conductivity of the region . Properties in each subdomain are constant but different from other subdomains. Subscripts of 1, 2, 3 and 4 are used to show the features of the healthy tissue, cancerous tissue, SPMs, and PCMs, respectively. Also, subscripts 5 and 6 are used to show the effective properties of the cancerous tissue filled with SPM particles and the effective properties of healthy tissue filled with PCM particles. The heat generated in the tumor tissue with SPM could be gained using [16]:

$$Q_r = \left[\frac{3n_3 r_3^3 \chi''}{4\mu_0 f R^2} + (1-\eta_3)\frac{\sigma_5}{2}\right].\left[|E_x|^2 + |E_y|^2\right] \quad (x,y) \in \Omega_2. \tag{5}$$

where μ_0 is the permeability of the free space ($\mu_0 = 4\pi\times10^{-7}\ \mathrm{T\cdot m\cdot A^{-1}}$), f is the frequency of the electromagnetic field, R is the radius of the magnetic induction loop, χ'' is the susceptibility of electromagnetic nanoparticles, σ_5 is the effective electrical conductivity in the tumor tissue, $\eta_3 = 4\pi n_3 r_3^3 / 3$ is the SPM ratio in a volume of tissue, r_3 is the radius of the SPM micro/nanoparticles, and n_3 is the concentration of the SPM micro/nanoparticles in the tumor tissue.

Pennes equation determines the temperature distribution within the tissue [14]:

$$\begin{aligned} c\frac{\partial T(x,y,t)}{\partial t} &= \nabla\cdot\left(k(x,y)\nabla T(x,y,t)\right) \\ &-\omega_b(x,y)c_b T(x,y,t) + \omega_b(x,y)c_b T_a \\ &+Q_m(x,y,t) + Q_r(x,y,t) \quad (x,y)\in\Omega. \end{aligned} \tag{6}$$

where Ω is the solution domain, c and c_b are the heat capacity of the tissue and blood respectively, T_a is the temperature of the supplier artery which is assumed to be constant, T is the temperature of tissue, k is the thermal conductivity, ω_b is the blood perfusion, Q_m is the heat generation and resulted from the body metabolism, and Q_r is the heat source comes from the electromagnetic field.

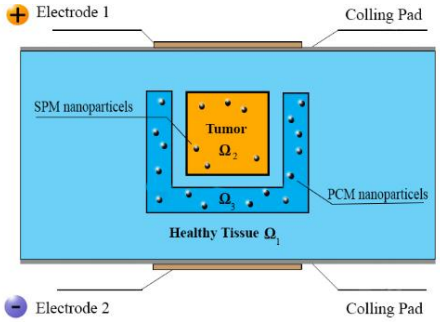

Figure 1. The regions of healthy tissue without PCM Ω_1, tumor with SPM Ω_2, and healthy tissue with PCMs Ω_3

The heat capacity c_4 and the thermal conductivity k_4 are estimated by [14]:

$$c_4 = \begin{cases} c_{4s}, & T < T_s \\ \dfrac{Q_l}{(T_l - T_s)} + \dfrac{c_{4s}+c_{4l}}{2}, & T_s \le T \le T_l \\ c_{4l}, & T > T_s \end{cases} \tag{7}$$

$$k_4 = \begin{cases} k_{4s}, & T < T_s \\ \dfrac{k_{4s}+k_{4l}}{2}, & T_s \le T \le T_l \\ k_{4l}, & T > T_s \end{cases} \tag{8}$$

where c_{4s}, c_{4l}, k_{4s}, and k_{4l} are the heat capacity of liquid and solid PCM, the thermal conductivity of liquid and solid PCM, respectively, and Q_l indicates the latent heat of the PCM [14]. Also, the effective electrical and thermal properties of the tissues with SPMs and PCMs are estimated as follows [9]:

$$\begin{aligned} c_2 &= (1-\eta_5)c_4 + \eta_5 c_5, \quad (x,y)\in\Omega_2 \\ c_3 &= (1-\eta_6)c_1 + \eta_6 c_6, \quad (x,y)\in\Omega_3 \end{aligned} \tag{9}$$

$$\begin{aligned} k_2 &= \left(\frac{1-\eta_5}{k_1} + \frac{\eta_5}{k_5}\right)^{-1}, \quad (x,y)\in\Omega_2 \\ k_3 &= \left(\frac{1-\eta_6}{k_1} + \frac{\eta_6}{k_6}\right)^{-1}, \quad (x,y)\in\Omega_3 \end{aligned} \tag{10}$$

$$\begin{aligned} \sigma_2 &= \left(\frac{1-\eta_5}{\sigma_4} + \frac{\eta_5}{\sigma_5}\right)^{-1}, \quad (x,y)\in\Omega_2 \\ \sigma_3 &= \left(\frac{1-\eta_6}{\sigma_1} + \frac{\eta_6}{\sigma_6}\right)^{-1}, \quad (x,y)\in\Omega_3 \end{aligned} \tag{11}$$

The boundary conditions for Equation (6) are defined as follows [14]:

$$\begin{aligned} -k\frac{\partial T}{\partial y} &= h_f(T_f - T), \quad y = 0\ \mathrm{m},\ y = 0.04\ \mathrm{m}, \\ -k\frac{\partial T}{\partial x} &= 0 \qquad\qquad x = 0\ \mathrm{m},\ x = 0.08\ \mathrm{m}. \end{aligned} \tag{12}$$

where h_f is the heat convection coefficient between the surface of the skin and water and T_f is the temperature of

the water. The details of discretization of equations and temperature distribution in the tissue are given in literature [22, 23], and the uncertainty analysis of thermal protection using PCM is studied here.

3. UNCERTAINTY ANALYSIS

The errors occur in the measurement of parameters are one of the important reasons that cause the difference between the results of the numerical results and the laboratory ones. Generally, the temperature could be defined by [17]:

$$T = f(w_1, w_2, ..., w_m) \tag{13}$$

where $w_1, w_2, \ldots, w_m$ indicate m parameters in the problem. Accordingly, the total uncertainty for temperature of the tissue can be obtained using the following equation [17]:

$$\Delta T = \sqrt{\left(\frac{\partial f}{\partial w_1}\Delta w_1\right)^2 + \left(\frac{\partial f}{\partial w_2}\Delta w_2\right)^2 + \ldots + \left(\frac{\partial f}{\partial w_m}\Delta w_m\right)^2} \tag{14}$$

where $\frac{\partial f}{\partial w}$ and Δw are the sensitivity coefficient and the uncertainty of the parameter, respectively.

4. NUMERICAL SOLUTION

Pennes Biothermal equation can be discretized by the finite difference method with a second-order accuracy considering $\Delta x = \Delta y$.

$$T_{i,j}^{s+1} = Fo\left(T_{i+1,j}^{s} + T_{i-1,j}^{s} + T_{i,j+1}^{s} + T_{i,j-1}^{s}\right) + (1 - 4Fo - W)T_{i,j}^{s} + \frac{\Delta t}{c}Q \tag{15}$$

where s denotes the time increment, $Fo = k\Delta t / c\Delta x^2$ is the Fourier number and $W = \omega_b c_b \Delta t / c$. Also, the discretized form of the boundary conditions are written as follows:

$$\begin{aligned} &T_{i,1}^{s} = \left(\frac{h_f \Delta x T_f}{k_1} + T_{i,2}^{s}\right) / \left(1 + \frac{h_f \Delta x T_f}{k_1}\right), \\ &T_{i,N}^{s} = \left(\frac{h_f \Delta x T_f}{k_1} + T_{i,N-1}^{s}\right) / \left(1 + \frac{h_f \Delta x T_f}{k_1}\right), \\ &T_{1,j}^{s} = T_{2,j}^{s}, \\ &T_{M,j}^{s} = T_{M-1,j}^{s}. \end{aligned} \tag{16}$$

The average of absolute error in each iteration (p) for the potential equation [28] is computed by.

$$\varepsilon^p = \frac{\sum_{i=1}^{M}\sum_{j=1}^{N}\left|T_{i,j}^{p+1} - T_{i,j}^{p}\right|}{M \times N} \tag{17}$$

The calculations stop, if the average of the absolute error falls below the concurrency criterion of 10^{-6}. The mesh independency is investigated for the temperature difference between two cases, tissue with PCM and tissue without PCM. For the same condition, Figure 2a displays the temperature difference on the vertical lines passing through the x=0.02 m and x=0.04 m and Figure 2b plots the temperature differences on the horizontal lines passing through the y=0.01 m and y=0.02 m for dx=0.0008 (101×51), dx=0.0005 (161×81), dx=0.0004 (201×101), and t= 500 seconds. As can be seen, with the change in the mesh resolution, the results do not change significantly, which results in mesh independency of the numerical results. Numerical validation has already been performed by the authors [19] for $R = 4.2\times10^{-8}\,m$ and $n = 4.8\times10^{6}\,m$ [15]. Figure 3 shows the flowchart for implementation of the numerical process.

5. RESULTS AND DISCUSS

The solution domain is rectangular with a dimension of 0.08×0.04 m^2. The heating area Ω_h is limited to 0.032 ≤ x≤.048 m, y=0 and 0.032 ≤x≤0.048m, y=0.04 m, and tumor area Ω_2 is limited to 0.032 ≤ x≤.048 m, 0.16 ≤ y≤.048m. The PCM area Ω_3 is specified in Table 1.

It is recognized that the presence of malignant tumor in the tissue changes the blood perfusion, heat capacity and heat of metabolism in the region of the tumor. For the healthy tissue and tissue with the tumor the magnetic and thermal properties are reported in Table 2. Also, the blood temperature is T_a=37 °C and the heat capacity of blood is c_b=4200 $kJ/m^3.K$. The boundary condition on the surface of the skin is the third kind with h_f =45 $W/m^2.K$ and T_f=20 °C, and other boundary conditions are assumed to be insulated [18]. The radius of the magnitude induction loop is R=0.01 m, voltage of the electrodes is U=8 V, and frequency of the electromagnetic domain is f=1 MHz. The thermophysical and electrical properties of the SPM and PCM are reported in Table 3. The susceptibility of electromagnetic nanoparticles is $\chi'' = 18$. Experimental results show that the nanoparticle size for cancer treatment should ideally be in the range of 10 to 100 nm [29].

The difference of temperature distribution between two cases, tissue with PCM and tissue without PCM is shown in Figure 4. According to this figure, it is observed that the injection of the PCM reduces the tissue temperature by more than 2 degrees, which justifies the use of PCM to control the temperature of the tissue during the hyperthermia.

To investigate the uncertainty analysis, a 20% tolerance has been assumed for each parameter. The positive or negative value of the uncertainty is so chosen to have the worst effect on thermal protection. Therefore

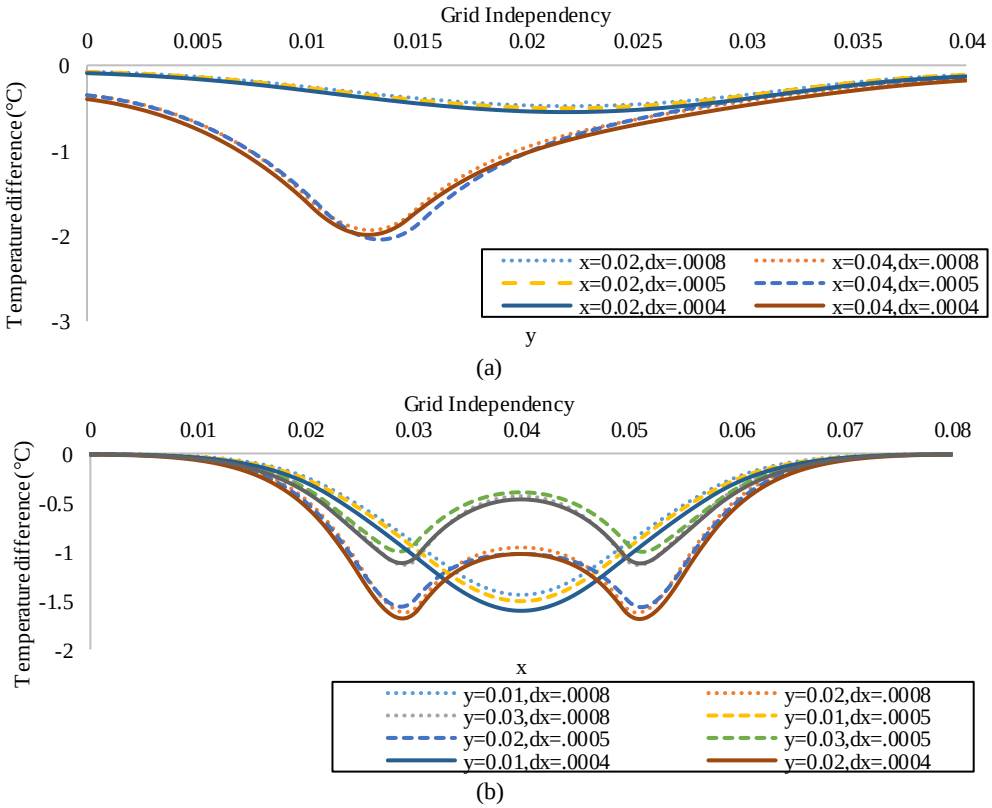

Figure 2. Investigation of the mesh independency at t=500 s for a) sections along the *x*-axis and b) sections along the *y*-axis

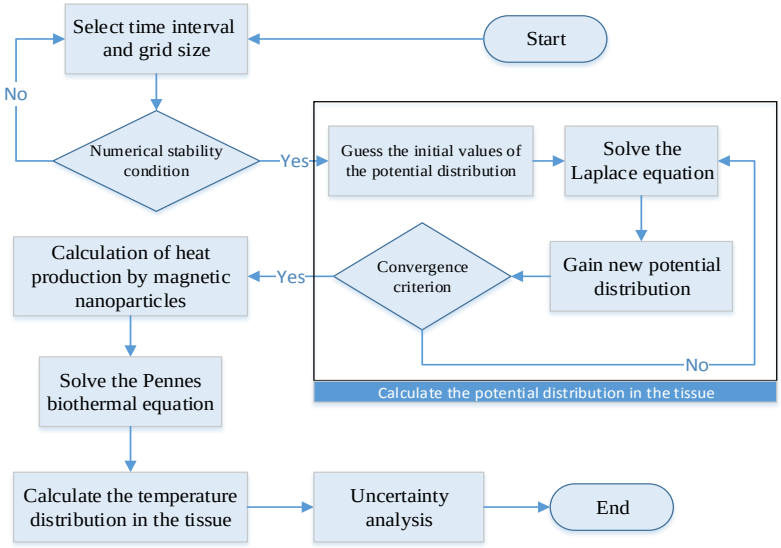

Figure 3. Flowchart of the numerical process for reaching the uncertainty analysis

TABLE 1. The area in which the PCM is injected into the tissue

$\Omega_3 = A \cap \overline{B}$
$A = \{(x, y) \mid 0.022 \le x \le 0.058 \text{ m}, 0.011 \le y \le 0.032 \text{ m}\}$
$B = \{(x, y) \mid 0.03 \le x \le 0.05 \text{ m}, 0.015 \le y \le 0.032 \text{ m}\}$

TABLE 2. Magnetic and thermal properties of healthy tissue and tissue with tumor [18]

	k (W/m.K)	c (J/m^3.K)	σ (S/m)	ω_b (1/s)	Q_m (W/m^3)
Healthy tissue	0.5	4.2×10^6	0.4	0.0005	4200
Tissue with tumor	0.6	4.2×10^6	0.48	0.002	42000

TABLE 3. Thermophysical and electrical properties of SPM and PCM [14]

	k (W/m.K)	c (J/m^3.K)	σ (S/m)	T_s (°C)	T_l (°C)	Q_l (J/m^3)	r (nm)	n (m^{-3})
SPM	40	2.072×10^7	25000	---	---	---	10	1×10^{19}
PCM	k_s=0.35 k_l=0.1	$c_s=2.56\times10^6$ $c_l=2.2\times10^6$	10^{-11}	38	42	1×10^8	10	1×10^{23}

all uncertainty values for the PCM are selected negative except the melting temperature, and uncertainty values for the SPM are selected positive. The uncertainty analysis of the concentration of micro/nanoparticles is shown in Figure 5. It is seen that the maximum temperature change in this case is only 0.22 °C, which is negligible.

The uncertainty analysis for the radius of the microcapsules is shown in Figure 6. The micro-capsulation of phase-change micro/nanoparticles should be in such a way that their radius not to be lower than the numerical value. It is seen that the difference from the numerical values is not perceptible so that a change of 20% of this parameter can affect the temperature distribution by about 0.5˚C.

Figure 7 shows the uncertainty analysis of the latent heat estimation. It is seen that a small deviation from the numerical values would not affect the results, and its impact can be ignored.

Uncertainty analysis of the melting temperature of micro/nanoparticles is shown in Figure 8. According to this figure, an imprecise estimation of the melting temperature affects the thermal protection over 1.1 °C. Hence to gain a similar results between the numerical and experimental data, the melting temperature should be estimated more accurately.

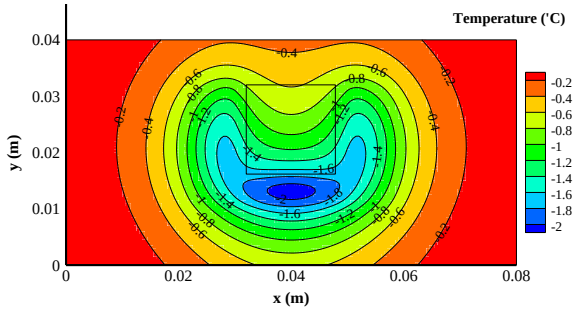

Figure 4. The difference of temperature distribution between two cases, tissue with PCM and tissue without PCM

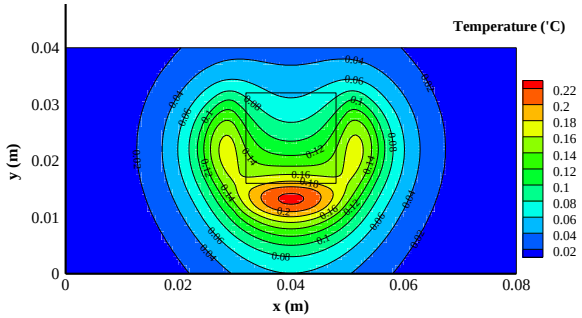

Figure 5. Temperature changes in the tissue due to a 20% change in the PCM concentration

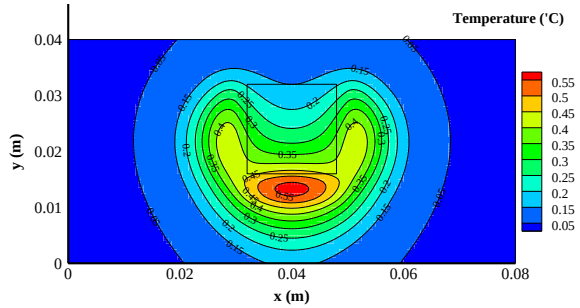

Figure 6. Temperature changes in the tissue due to a 20% change in the micro-capsulation radius of the PCM

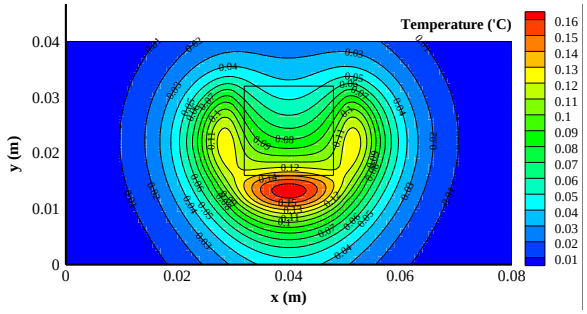

Figure 7. Temperature changes in the tissue due to a 20% change in the latent heat of the PCM

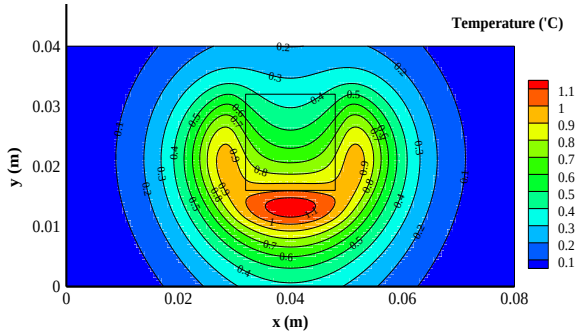

Figure 8. Temperature changes in the tissue due to a 20% change in the melting temperature of the PCM

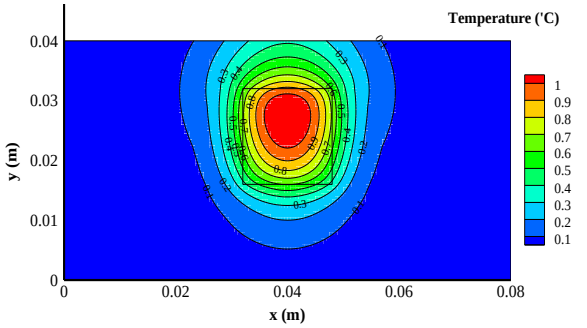

Figure 10. Temperature changes in the tissue due to a 20% change in the concentration of the SPM

Figure 9 shows the temperature changes in the tissue due to a 20% changes in the, solidus and liquidus temperatures of the phase-change micro/nanoparticles (the range of phase-change). Based on this figure, the deviation from the numerical values for the solidus and liquidus temperatures is so small, and there is no sensitivity to determine it precisely in the laboratory. As was shown in the previous study [23], the concentration and radius of SPM can also affect the thermal protection of the healthy tissue during the hyperthermia, thus the uncertainty analysis for these parameters are presented.

Figure 10 shows the temperature changes after 20% change of the concentration of the SPM. According to this figure, any small deviation from numerical values is negligible because the temperature change in the healthy tissues around the tumor is not significant.

Uncertainty of the radius of the SPM micro/nanoparticles has increased the temperature in the tumor tissue and also in the healthy tissues about 4˚C and 3˚C, respectively. This shows that the radius of the SPM micro/nanoparticles should be estimated accurately. The uncertainty of the radius of SPM micro/nanoparticles is shown in Figure 11. A summary of uncertainty analyzes is given in Table 4. These results are also graphically plotted in Figure 12.

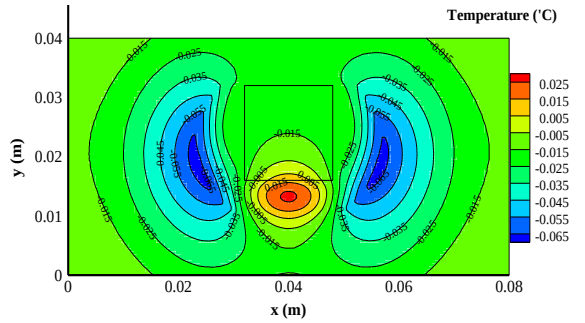

Figure 9. Temperature changes in the tissue due to a 20% change in the solidus and liquidus temperatures of the PCM

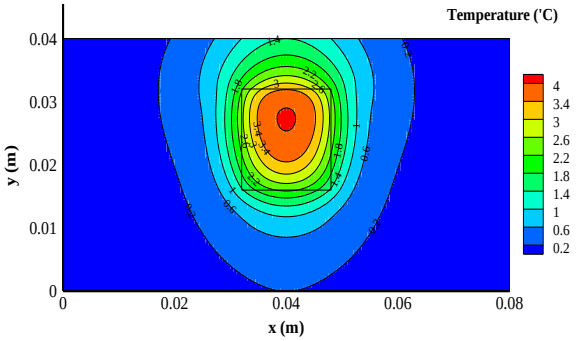

Figure 11. Temperature changes in the tissue due to a 20% change in the radius of the SPM

TABLE 4. Temperature variations in the tissue due to 20% changes in effective parameter at t=1000 (s)

Region	Maximum Temperature variation ˚C						
	Concentration of the PCM	Micro-capsulation radius of the PCM	Latent heat of the PCM	Melting temperature of the PCM	Range of solidus and liquidus temperatures of the PCM	Concentration of the SPMs	Radius of the SPM
Healthy tissue	0.22	0.47	0.17	1.15	0.065	0.6	3.2
Tumor tissue	0.17	0.57	0.14	0.98	0.025	1.12	4.1

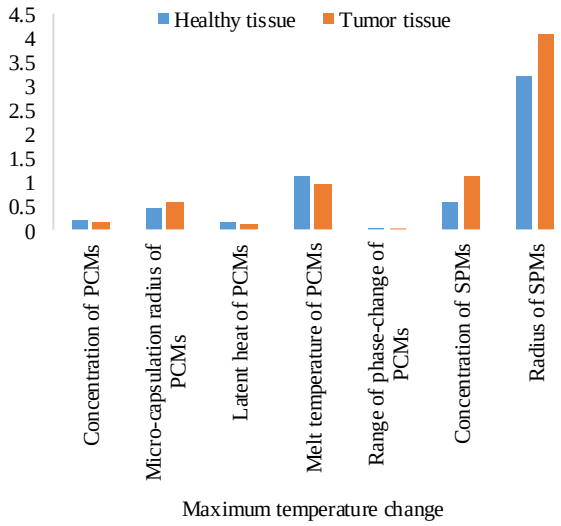

Figure 12. Temperature variations in the tissue due to 20% changes for the effective parameters at t=1000 (s)

6. CONCLUSION

In the present study, the inevitable deviation of the laboratory values with the numerical ones is investigated for the SPM and PCM. The results show that the deviation of some quantities affect the protection of healthy tissues during the hyperthermia and therefore need more precision in measurement of parameters for the practical condition. According to the obtained results, the deviation of the concentration, the radius of micro-capsulation, the latent heat and the range of the melting temperature have no significant effect on the thermal protection of healthy tissues. But the melting temperature of the PCM, the concentration of the SPM and the radius of SPM must be measured more accurately to gain the equal numerical and experimental results.

According to the results, a 20% difference between the numerical and laboratory values can cause a significant temperature change in the tissue. Uncertainties in measuring the concentration of the PCM, the radius of the micro-capsulation, the latent heat of the PCM, the melting temperature, the concentration of the SPM, and the radius of the SPM cause temperature change about 0.22 °C, 0.55 °C, 0.16 °C, 1.1 °C, 1 °C and 4 °C, respectively. Therefore, the radius of the SPM, the melting temperature and the concentration of the SPM should be more accurately measured.

7. REFERENCES

1. Zendehdel, K., "Cancer statistics in ir iran in 2018", ***Basic & Clinical Cancer Research***, Vol. 11, No. 1, (2019). https://doi.org/10.18502/bccr.v11i1.1645.
2. Pala, T., Ycedag, I. and Biberoglu, H., "Association rule for classification of breast cancer patients", ***Sigma Journal of Engineering and Natural Sciences***, Vol. 8, No. 2, (2017), 155-160.
3. Ozkan, E., Erdemir, A., Torer, B.D., Tasci, A.I., Baskin, Y., Ellidokuz, H. and Balik, D.T., "Genotyping and analysis of rs7501939 polymorphism for prostate cancer", ***Sigma Journal of Engineering and Natural Sciences***, Vol. 6, No. 1, (2015), 101-107.
4. Kizilbey, K. and Akdeste, Z.M., "Melanoma cancer", ***Sigma Journal of Engineering and Natural Sciences***, Vol. 31, No. 4, (2013).
5. Cabuy, E., "Reliable cancer therapies", ***Energy-Based Therapies. Hyperthermia in Cancer Treatment, RCT Summary for Professionals***, Vol. 1, No. 2, (2011), 1-48.
6. van der Zee, J., González, D., van Rhoon, G.C., van Dijk, J.D., van Putten, W.L. and Hart, A.A., "Comparison of radiotherapy alone with radiotherapy plus hyperthermia in locally advanced pelvic tumours: A prospective, randomised, multicentre trial", ***The Lancet***, Vol. 355, No. 9210, (2000), 1119-1125. https://doi.org/10.1016/s0140-6736(00)02059-6.
7. Pirouz, F., Najafpour, G., Jahanshahia, M. and Sharifzadeh Baei, M., "Plant-based calcium fructoborate as boron-carrying nanoparticles for neutron cancer therapy", ***International Journal of Engineering, Transactions A: Basics***, Vol. 32, No. 4, (2019), 460-466. https://dx.doi.org/10.5829/ije.2019.32.04a.01.
8. Falk, M. and Issels, R., "Hyperthermia in oncology", ***International Journal of Hyperthermia***, Vol. 17, No. 1, (2001), 1-18. https://doi.org/10.1080/02656730118511.
9. Javadi, K. and Komjani, N., "Investigation into low sar pifa antenna and design a very low sar u-slot antenna using frequency selective surface for cell-phones and wearable applications", ***Emerging Science Journal***, Vol. 1, No. 3, (2017), 145-157. https://doi.org/10.28991/ijse-01117.
10. Zhang, S., Clark, M., Liu, X., Chen, D., Thomas, P. and Ren, L., "The effects of bio-inspired electromagnetic fields on healthy enhancement with case studies", ***Emerging Science Journal***, Vol. 3, No. 6, (2019), 369-381. https://doi.org/10.28991/esj-2019-01199.
11. Priscilla, S.J., Judi, V.A., Daniel, R. and Sivaji, K., "Effects of chromium doping on the electrical properties of zno nanoparticles", ***Emerging Science Journal***, Vol. 4, No. 2, (2020), 82-88. https://doi.org/10.28991/esj-2020-01212.
12. Manikandan, G., Yuvashree, M., Sangeetha, A., Bhuvana, K. and Nayak, S.K., "Liver tissue regeneration using nano silver impregnated sodium alginate/pva composite nanofibres", ***SciMedicine Journal***, Vol. 2, No. 1, (2020), 16-21. https://doi.org/10.28991/SciMedJ-2020-0201-3.
13. Puspitasari, P. and Budi, L., "Physical and magnetic properties comparison of cobalt ferrite nanopowder using sol-gel and sonochemical methods", ***International Journal of Engineering, Transactions B: Applications***, Vol. 33, No. 5, (2020), 877-884. https://dx.doi.org/10.5829/ije.2020.33.05b.20.
14. Lv, Y., Zou, Y. and Yang, L., "Theoretical model for thermal protection by microencapsulated phase change micro/nanoparticles during hyperthermia", ***Heat and Mass Transfer***, Vol. 48, No. 4, (2012), 573-584. https://doi.org/10.1007/s00231-011-0907-4.
15. Sezgin, E., Karatas, O., Çam, D., Sur, İ., Sayin, İ. and Avci, E., "Interaction of gold nanoparticles with living cells", ***Sigma***, Vol. 26, (2008), 227-246.
16. Lv, Y.-G., Deng, Z.-S. and Liu, J., "3-d numerical study on the induced heating effects of embedded micro/nanoparticles on human body subject to external medical electromagnetic field",

IEEE Transactions on Nanobioscience, Vol. 4, No. 4, (2005), 284-294. https://doi.org/10.1109/TNB.2005.859549.

17. Deng, Z.-S. and Liu, J., "Uncertainties in the micro/nano-particles induced hyperthermia treatment on tumor subject to external em field", in 2006 1st IEEE International Conference on Nano/Micro Engineered and Molecular Systems, IEEE, (2006), 851-855. https://doi.org/10.1109/NEMS.2006.334910.
18. Majchrzak, E., Dziatkiewicz, G. and Paruch, M., "The modelling of heating a tissue subjected to external electromagnetic field", ***Acta of Bioengineering and Biomechanics***, Vol. 10, No. 2, (2008), 29-37. PMID: 19031995.
19. Majchrzak, E. and Paruch, M., "Numerical modelling of temperature field in the tissue with a tumor subjected to the action of two external electrodes", ***Scientific Research of the Institute of Mathematics and Computer Science***, Vol. 8, No. 1, (2009), 137-145.
20. Majchrzak, E. and Paruch, M., "Application of evolutionary algorithms for identification of number and size of nanoparticles embedded in a tumor region during hyperthermia treatment", Evolutionary and Deterministic Methods for Design, Optimization and Control with Applications to Industrial and Societal Problems (eds. T. Burczyński and J. Periaux), CIMNE, Barcelona, Spain, A Series of Handbooks on Theory and Engineering Applications of Computational Methods, (2011), 310-315.
21. Q. Zhao, L. Wang, R. Cheng, L. Mao, R.D. Arnold, E.W. Howerth, Z.G. Chen, S. Platt, Magnetic nanoparticle-based hyperthermia for head & neck cancer in mouse models, ***Theranostics***, Vol. 2, No. 1, (2012). https://doi:10.7150/thno.3854.
22. F. Talati, A.A. Taheri, Numerical study of induction heating by micro/nano magnetic particles in hyperthermia, ***Journal of Computational & Applied Research in Mechanical Engineering (JCARME)***, (2019). https://doi.org/10.22061/JCARME.2019.3961.1465.
23. Talati, F. and Taheri, A.A., "Uncertainty analysis in induction heating by magnetic micro/nanoparticles during hyperthermia", ***Journal of Mechanical Engineering***, Vol. 48, No. 4, (2019), 195-201.
24. Taheri, A.A. and Talati, F., "Fdm-based 2d numerical study of hyperthermia cancer treatment by micro/nano-phase-change materials", ***Iranian Journal of Science and Technology, Transactions of Mechanical Engineering***, (2019), 1-13. https://doi.org/10.1007/s40997-019-00314-y.
25. Nemati, Z., Alonso, J., Martinez, L., Khurshid, H., Garaio, E., Garcia, J., Phan, M. and Srikanth, H., "Enhanced magnetic hyperthermia in iron oxide nano-octopods: Size and anisotropy effects", ***The Journal of Physical Chemistry C,*** Vol. 120, No. 15, (2016), 8370-8379. https://doi.org/10.1021/acs.jpcc.6b01426.
26. Wang, H., Dai, W. and Bejan, A., "Optimal temperature distribution in a 3d triple-layered skin structure embedded with artery and vein vasculature and induced by electromagnetic radiation", ***International Journal of Heat and Mass Transfer,*** Vol. 50, No. 9-10, (2007), 1843-1854. https://doi.org/10.1016/j.ijheatmasstransfer.2006.10.005.
27. Li, L., Yu, B., Liang, M., Yang, S. and Zou, M., "A comprehensive study of the effective thermal conductivity of living biological tissue with randomly distributed vascular trees", ***International Journal of Heat and Mass Transfer,*** Vol. 72, (2014), 616-621. https://doi.org/10.1016/j.ijheatmasstransfer.2014.01.044.
28. Ferziger, J.H. and Perić, M., "Computational methods for fluid dynamics, Springer, Vol. 3, (2002).
29. Kazemi, S., Rezaei, S., Mohammadi, M. and Nikzad, M., "Separation of curcumin from curcuma longa l. And its conjugation with silica nanoparticles for anti-cancer activities", ***International Journal of Engineering, Transactions C: Aspects***, Vol. 31, No. 9, (2018), 1803-1809.

Persian Abstract

چکیده

در محافظت گرمایی از بافت‌های سالم در طول هایپرترمیا به‌وسیله مواد میکرو/نانو تغییر فاز دهنده (PCM)، انحراف از مقادیر نظری در شرایط آزمایشگاهی به دلیل خطاهای مختلف مانند مدلسازی، اندازه‌گیری، جابجایی ذرات و غیره اجتناب‌ناپذیر است. این انحراف‌ها می‌توانند محافظت گرمایی عملی را با آسیب به سلولهای سالم یا عدم تخریب سلولهای تومور تحت تأثیر قرار دهند. برای انجام روش عددی، با استفاده از روش اختلاف محدود، توزیع پتانسیل با حل معادله لاپلاس و برای یافتن توزیع دما در بافت معادله زیست گرمایی پنس استفاده شده است. معادله پنس با در نظر گرفتن رسانش درون بافت، پرفیوژن خون و گرمای متابولیک بدن به صورت گذرا حل شده است. در نتیجه انحراف و عدم قطعیت هر یک از عوامل موثر در محافظت گرمایی شامل غلظت مواد تغییر فاز دهنده، شعاع میکروکپسوله کردن، گرمای نهان، دمای ذوب و گستره تغییر فاز میکرو/ نانوذرات تغییر فاز دهنده و همچنین تأثیر غلظت و شعاع مواد سوپر پارامغناطیس (SPM) بررسی شده است. مطابق نتایج به دست آمده از آنالیز عدم قطعیت، شعاع SPMs پر اهمیت ترین پارامتر است و انحراف ۲۰ ٪ از مقدار عددی این پارامتر میتواند تا میزان ٤ درجه سیلسیوس بر روی دمای بافت تاثیرگذار باشد.